Journal of Chromatography A, 1217 (2010) 6531–6544

Contents lists available at ScienceDirect

Journal of Chromatography A

journal homepage: www.elsevier.com/locate/chroma

Impurity profiling of acetylspiramycin by liquid chromatography–ion trap mass spectrometry

Ming-juan Wang[a,b], Murali Pendela[b], Chang-qin Hu[a], Shao-hong Jin[a], Jos Hoogmartens[b], Ann Van Schepdael[b], Erwin Adams[b,*]

[a] National Institute for Control of Pharmaceutical and Biological Products, Beijing 100050, China
[b] Katholieke Universiteit Leuven, Faculteit Farmaceutische Wetenschappen, Laboratorium voor Farmaceutische Analyse, O&N2, PB 923, Herestraat 49, B-3000 Leuven, Belgium

ARTICLE INFO

Article history:
Received 25 May 2010
Received in revised form 15 July 2010
Accepted 23 August 2010

Keywords:
Liquid chromatography/tandem mass spectrometry
16-Membered macrolide
Acetylspiramycin
Impurity profile

ABSTRACT

Investigation of acetylspiramycin (ASPM) and its related substances was carried out using a reversed-phase liquid chromatography/tandem mass spectrometry method. The identification of impurities in the ASPM complex was performed with a quadrupole ion trap mass spectrometer, with an electrospray ionization (ESI) source in the positive ion mode which provides MS^n capability. A total of 83 compounds were characterized in commercial samples, among which 31 impurities that had never been reported and 31 partially characterized impurities were deduced using the collision-induced dissociation (CID) spectra of major ASPM components as templates. Most of the major impurities arise from the starting materials and the synthesis process. This work provides very useful information for quality control of ASPM and evaluation of its synthesis process.

1. Introduction

Acetylspiramycin (ASPM), a 16-membered macrolide antibiotic, is the acetylated derivative of spiramycin (SPM). Due to different producing strains, SPM produced in China is usually composed of SPM II and III, whereas the major component of SPM produced in Europe is SPM I. Thus, ASPM synthesized from SPM in China generally contains four major components (mono-ASPM II/III, di-ASPM II/III) and other co-existing minor components [1,2]. The structures of ASPM and its known related substances, including starting materials (SPM I/II/III), synthetic intermediates (2′,4″-di-ASPM II/III, 2′,3″,4″-tri-ASPM II/III) and degradation products (3,4-anhydro NSPM I, NSPM I/II/III, leucomycin A8/U, meleumycin B2) [1–4], are shown in Fig. 1.

SPM is unstable in acidic conditions to produce neospiramycin (NSPM) and/or forosidin (which is formed by loss of mycarose and forosaminyl) [3], and the introduction of 4″-acyl groups in SPM enhanced the acid-stability. It was reported that SPM derivatives with longer carbon chains at position 3 or 4″ have better antibiotic activity due to their higher lipophilicity [3,5–8]. ASPM, which showed improved metabolic stability, was synthesized by Kyowa Hakko Kogyo Co. in 1965 and further introduced into clinical use [3]. Clinical studies have shown its efficacy against Gram-positive organisms including *Streptococcus pyogenes* (group A beta-hemolytic streptococci), *Streptococcus viridans*, *Corynebacterium diphtheriae* and methicillin-sensitive *Staphylococcus aureus* and also some Gram-negative bacteria such as *Neisseria meningitidis*, *Bordetella pertussis* and *Campylobacter* [9,10].

During the synthesis process of ASPM, the acetylation degree of final products can be influenced by reaction conditions. Higher temperature or longer reaction time can lead to higher acetylation degree, meanwhile increasing the risk of degradation of final products [1].

The impurity profile provides a comprehensive indicator of the synthesis process and is diagnostic of the overall quality of final products. In the current Chinese Pharmacopoeia (ChP), the ratio of major components is controlled, but without specifications for the related substances [11]. To further ensure the safety of commercial ASPM, it is necessary to characterize its impurities and establish proper limits for the related substances.

LC/ESI-MS provides a sensitive and selective procedure for the rapid identification of impurities. In this paper, we will focus on the characterization of impurities in ASPM using LC/ESI-MS^n. Based on the fragmentation pathway of SPM and some other macrolides [2–4,12], the LC–UV method described in the ChP for the ratio of major components [11] was combined with MS to identify impurities in commercial ASPM. This allows better evaluation of the synthesis process and quality control of ASPM and will enable future establishing of proper limits for the related substances.

* Corresponding author. Tel.: +32 16 323444; fax: +32 16 323448.
E-mail address: Erwin.Adams@pharm.kuleuven.be (E. Adams).

0021-9673/$ – see front matter © 2010 Elsevier B.V. All rights reserved.
doi:10.1016/j.chroma.2010.08.061

2. Experimental

2.1. Reagents and samples

Acetonitrile (LC/MS grade) was purchased from Biosolve (Valkenswaard, the Netherlands), ammonium acetate from Acros Organics (Geel, Belgium) and ammonium hydroxide solution (28%, m/m) from VWR (Leuven, Belgium). A Milli-Q water purification system (Millipore, Bedford, MA, USA) was used to purify deionized water.

Different batches of ASPM samples examined were obtained from Henan Topfond (Henan, China), Lukang Antibiotic Factory (Shandong, China), Suzhou Erye Pharmaceutical Factory (Jiangsu, China) and Baiyunshan Pharmaceutical Factory (Guang-

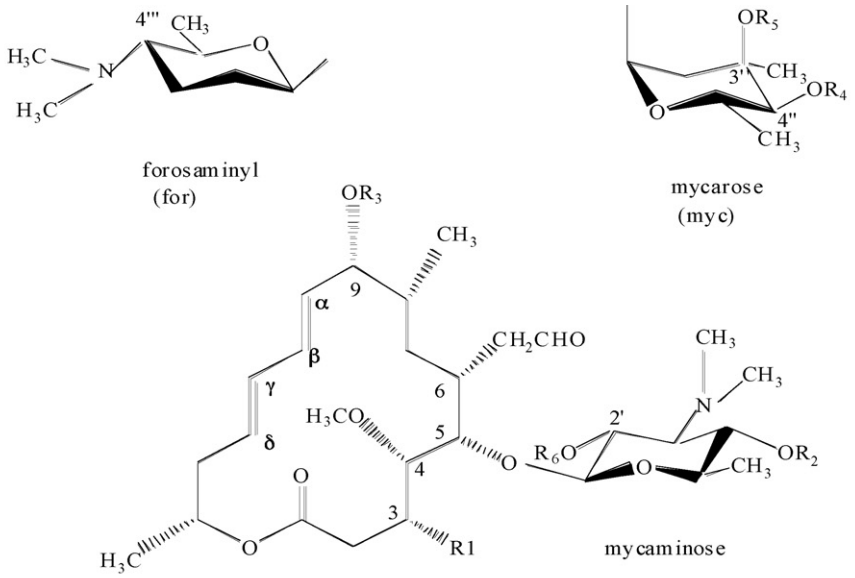

	$[M+H]^+$	R1	R2	R3	R4	R5	R6	Comment [1)]
mono-ASPM II	927	$OCOCH_3$	myc	for	$COCH_3$	H	H	Major components
mono-ASPM III	941	$OCOCH_2CH_3$	myc	for	$COCH_3$	H	H	[1-2]
di-ASPM II	969	$OCOCH_3$	myc	for	$COCH_3$	$COCH_3$	H	
di-ASPM III	983	$OCOCH_2CH_3$	myc	for	$COCH_3$	$COCH_3$	H	
mono-ASPM I	885	OH	myc	for	$COCH_3$	H	H	Minor components
di-ASPM I	927	OH	myc	for	$COCH_3$	$COCH_3$	H	[1]
SPM I [2)]	843	OH	myc	for	H	H	H	Starting materials
SPM II	885	$OCOCH_3$	myc	for	H	H	H	[1,4]
SPM III	899	$OCOCH_2CH_3$	myc	for	H	H	H	
2′,4″-di-ASPM II	969	$OCOCH_3$	myc	for	$COCH_3$	H	$COCH_3$	Synthetic
2′,4″-di-ASPM III	983	$OCOCH_2CH_3$	myc	for	$COCH_3$	H	$COCH_3$	intermediates
2′,3″,4″-tri-ASPM II	1011	$OCOCH_3$	myc	for	$COCH_3$	$COCH_3$	$COCH_3$	[1]
2′,3″,4″-tri-ASPM III	1025	$OCOCH_2CH_3$	myc	for	$COCH_3$	$COCH_3$	$COCH_3$	
3,4-anhydro NSPM I [3)]	681	–	H	for	–	–	H	Degradation
NSPM I [2)]	699	OH	H	for	–	–	H	products
NSPM II	741	$OCOCH_3$	H	for	–	–	H	[2-4]
NSPM III	755	$OCOCH_2CH_3$	H	for	–	–	H	
leucomycin A8	786	$OCOCH_3$	myc	H	$COCH_3$	H	H	
leucomycin U [2)]	744	$OCOCH_3$	myc	H	H	H	H	
meleumycin B2	800	$OCOCH_2CH_3$	myc	H	$COCH_3$	H	H	

1) The references where the related substances were reported are shown in square brackets;

2) Not observed in the samples investigated;

3) Its stereochemistry will change correspondingly due to the formation of a double bond between C-3 and C-4.

Fig. 1. Chemical structures of ASPM and its known related substances.

dong, China). For LC/MS and LC/MS^n, bulk samples were prepared in mobile phase at a concentration of about 1.0 mg mL^{-1}.

2.2. LC-instrument and chromatographic conditions

The LC apparatus consisted of a Dionex P680 binary pump (Dionex, Sunnyvale, CA, USA), a Spectra Series AS100 autosampler equipped with a 20 μL loop, a variable wavelength TSP spectra 100 UV-VIS detector (ThermoFinnigan, Fremont, CA, USA) set at 232 nm and Chromeleon software (Dionex) for data acquisition. The CAPCELL PAK C_{18} column (type: MG, size: 250 × 4.6 mm i.d., 5 μm) (Shiseido, Japan) was maintained at room temperature.

A mobile phase containing acetonitrile–0.1 M ammonium acetate solution (pH 7.2, adjusted with ammonium hydroxide solution) (50:50, v/v) was used at a flow rate of 1.0 mL min^{-1}. One-fifth of the column eluent was sent into the MS for peak characterization by splitting through a T-piece.

2.3. LC/MS experiments

Tuning and MS investigation of the ASPM related substances were carried out according to the procedure described by Govaerts et al. [12].

The mass spectrometric conditions were as follows: ESI positive ionization mode, capillary temperature was 270 °C, spray voltage was 4.5 kV, the flow rates of the sheath and the auxiliary gas were set at 72 and 56 arb, respectively, full scan from 1100 to 300 u.

The acquisition of the first-order mass spectra as well as the LC–MS/MS and further MS^n collision-induced dissociation (CID) experiments were performed on ASPM sample solutions. For LC–MS/MS investigations, the ions of interest were isolated in the ion trap with an isolation width of 3 u and activated at 40% collision-energy level (CEL). Under such conditions, the highest signal of the product ions needed for further MS^n CID experiments was obtained.

3. Results and discussion

3.1. Liquid chromatographic method

The LC method for the separation of ASPM major components in the ChP (2005) [11] was tried on a CAPCELL PAK C_{18} column (type: MG, size: 250 × 4.6 mm i.d., 5 μm) and two Xterra MS C_{18} columns (size: 250 × 4.6 mm i.d., 5 μm and 3.5 μm, respectively). The CAPCELL PAK C_{18} gave the best result, in terms of both separation and peak shape. To further improve the separation, the relative percentage of acetonitrile was reduced from 60% to 50%, and other conditions were kept constant. The typical total ion chromatogram (TIC) and the LC–UV of a sample are shown in Fig. 2. For better visualization, the chromatogram was zoomed between 0–32 min and 32–120 min. In total, 56 peaks were observed, though some impu-

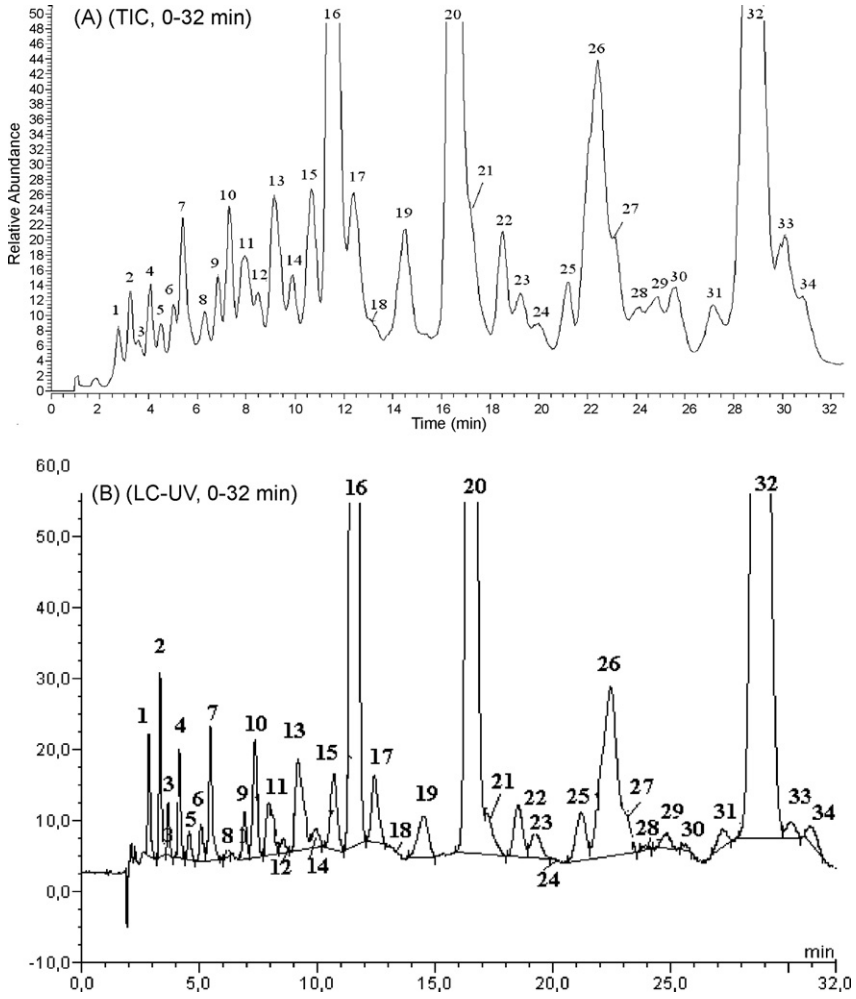

Fig. 2. Typical TIC– and LC–UV chromatograms of a commercial ASPM sample. (A) TIC (0–32 min), (B) LC–UV (0–32 min), (C) TIC (32–120 min), (D) LC–UV (32–120 min). Column: CAPCELL PAK C_{18} (type: MG, size: 250 × 4.6 mm i.d., 5 μm), maintained at room temperature. Mobile phase: acetonitrile–ammonium acetate solution (pH 7.2) (50:50, v/v). Flow rate: 1.0 mL min^{-1}. Sample concentration: ~1.0 mg mL^{-1}, injection volume: 20 μL.

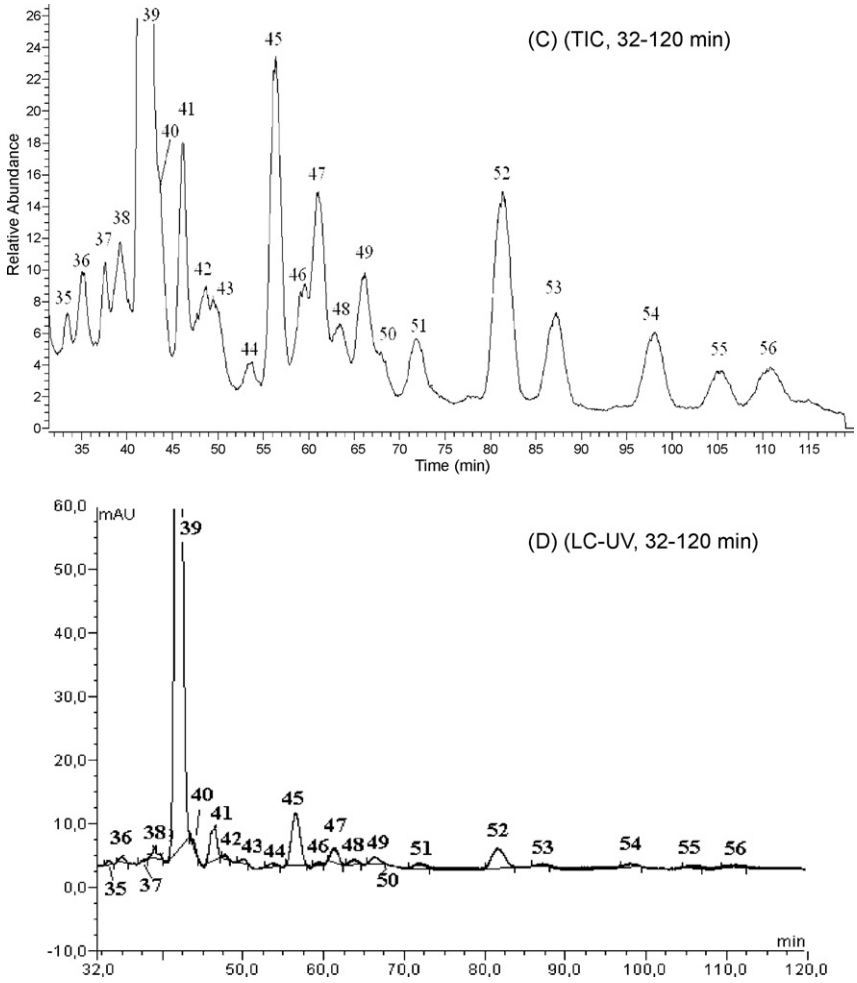

Fig. 2. (*Continued*).

rities were very small in the LC–UV chromatogram. Furthermore, peak purity for individual peaks was tested with the MS capability of extracted ion chromatograms. It was observed that some peaks in the TIC chromatogram of LC/MS are composed of more than two components. Further improvement of the separation would lead to even longer retention times and was not performed since MS has additional separation capability. The major components were eluted in the order of mono-ASPM II (peak 16), mono-ASPM III (peak 20), di-ASPM II (peak 32) and di-ASPM III (peak 39), in accordance with their hydrophobic order. The major impurity in all the samples investigated is peak 26 (normalized peak area percentage 2.9–3.8% by LC–UV).

3.2. Study of the fragmentation behavior of components with known structure

For a better understanding of the spectra of the impurities, initially the fragmentation behavior of the major ASPM components was studied. No doubly charged ions were observed under the used experimental conditions. The MS/MS spectra of the protonated molecules $[M+H]^+$ of the major components (mono-ASPM II: m/z 927, mono-ASPM III: m/z 941, di-ASPM II: m/z 969 and di-ASPM III: m/z 983) and their fragmentation pathway are shown in Figs. 3 and 4, respectively. As it can be seen, most product ions were formed by cleavage of the glycosidic bonds, in accordance with other macrolide antibiotics [2–4,12]. The consecutive neutral losses of 159, 186 or 228, and 191 corresponded to the cleavage of forosaminyl at C-9, mono-/di-acetylated mycarose and mycaminose at C-5, respectively. The presence of the characteristic disaccharide ion with m/z 360 or 402 further revealed that the corresponding mycarose was mono- or di-acetylated, respectively. Further fragmentation is in accordance with that of SPM II and III described by Pendela et al. [4].

The fragmentation patterns of minor components, e.g. mono-ASPM I (peak 13, $[M+H]^+$ m/z 885) and di-ASPM I (peak 25, $[M+H]^+$ m/z 927), are similar to those of the major components, which show consecutive neutral losses of 159, 186 or 228, and 191. Their further fragmentations of the aglycone ions at m/z 349, are in accordance with that of SPM I [4].

3.3. Investigation of components present in commercial ASPM samples

Based on the fragmentation behavior of the major ASPM components, the impurity profile of 11 commercial samples from four different origins were screened. The major ASPM components and most of the related substances in the investigated samples were similar in type, but their relative amounts varied slightly. The similarity of different batches of a same manufacturer indicated that their production processes are repeatable.

As ASPM is semi-synthetic, its impurities may arise from starting materials, synthesis process or degradation. The related substances will be discussed according to their source and structural differences compared to major ASPM components.

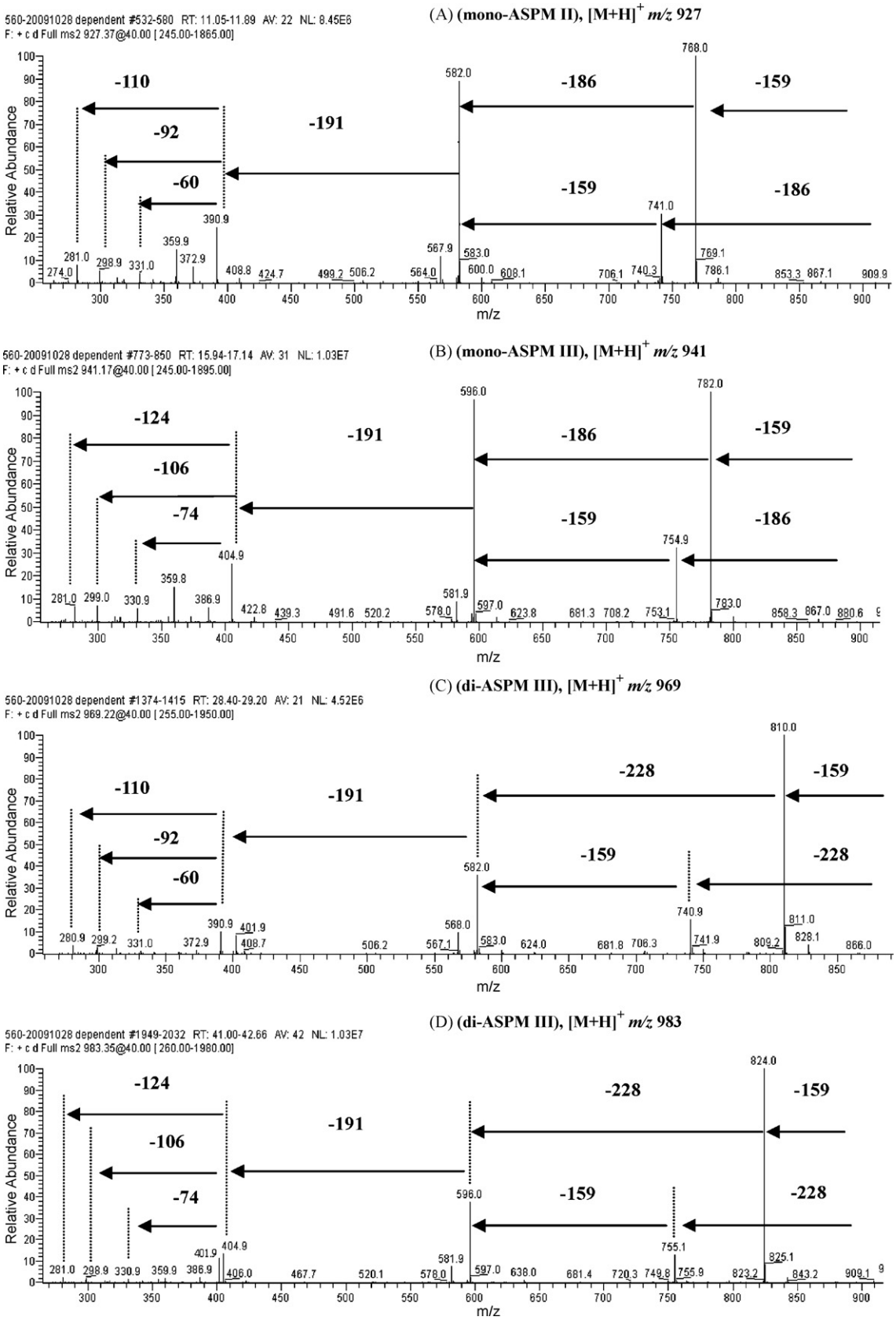

Fig. 3. $[M+H]^+$ CID spectra acquired for (A) mono-ASPM II, (B) mono-ASPM III, (C) di-ASPM II, and (D) di-ASPM III; the result of isolation and collisional activation in the ion trap at 40% CEL of the precursor ions at *m*/*z* 927, 941, 969 and 983, respectively.

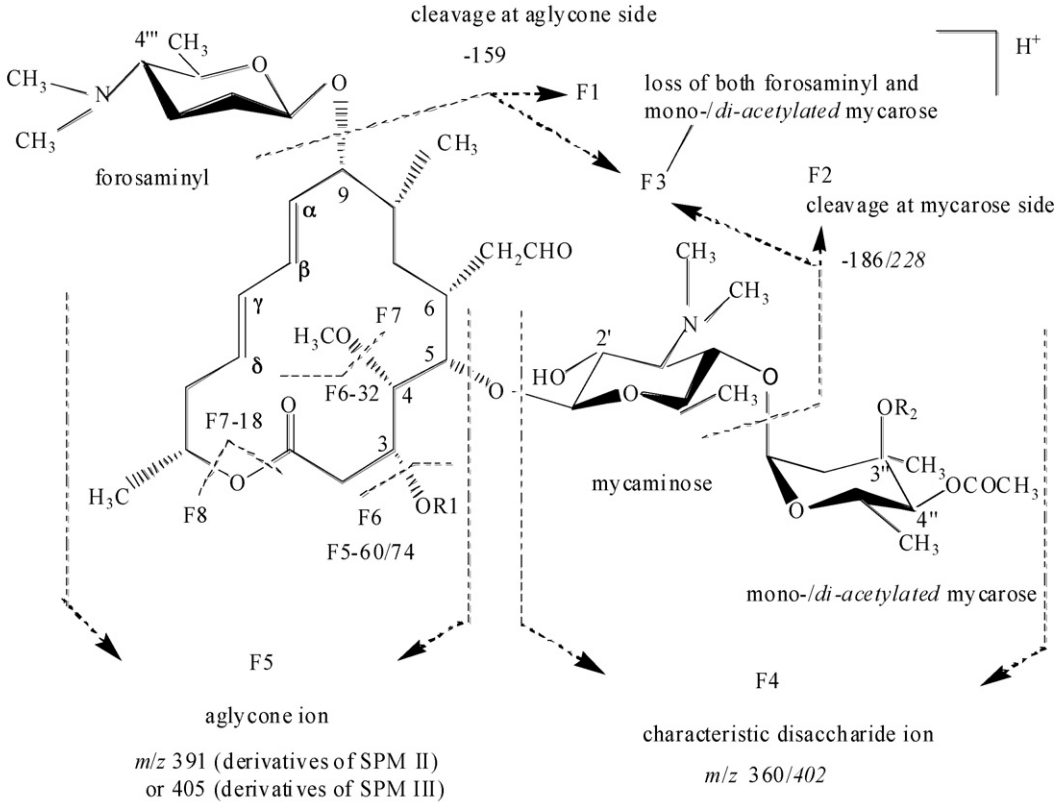

Compounds	R1	R2	$[M+H]^+$	F1	F2	F3	F4	F5	F6	F7	F8
Mono-ASPM II	$COCH_3$	H	927	768	741	582	360	391	331	299	281
Mono-ASPM III	$COCH_2CH_3$	H	941	782	755	596	360	405	331	299	281
di-ASPM II	$COCH_3$	$COCH_3$	969	810	741	582	402	391	331	299	281
di-ASPM III	$COCH_2CH_3$	$COCH_3$	983	824	755	596	402	405	331	299	281

Fig. 4. Fragmentation pathway of the major ASPM components. Values for the di-acetylated derivatives are given in italics.

3.3.1. Minor components from starting materials

Compounds corresponding to peak 7 ($[M+H]^+$ *m/z* 885) and peak 10 ($[M+H]^+$ *m/z* 899) were identified as SPM II and III, respectively, in accordance with the published results [4]. SPM I was not observed in the investigated samples, due to its low content in Chinese SPM products.

3.3.2. Synthesis process-related impurities

The $[M+H]^+$ CID spectra of peaks 27, 40, 47 and 52 at *m/z* 969, 983, 1011 and 1025 are illustrated in Fig. 5. The impurities in peaks 33, 34, 51 and 55 have the same *m/z* values and similar product ions to those of peaks 27, 40, 47 and 52, respectively. The consecutive losses of 159 and 186/228 revealed the presence of forosaminyl and mono- (peaks 27, 33, 40, 34)/di-acetylated (peaks 47, 51, 52, 55) mycarose. The observed loss of 233 instead of 191 in the above mentioned peaks indicates the cleavage of an aberrant mycaminose. Based on the synthesis process of ASPM, the above differences (+42 u) were attributed to acetylation at 2′-OH of mycaminose (see Fig. 1). The characteristic ion set of *m/z* 391/405, 331, 299 and 281 indicated they were derivatives of SPM II (peaks 27, 33, 47, 51) and III (peaks 40, 34, 52, 55), respectively. Based on the above information, they were identified as 2′,4″-di-ASPM II (peaks 27 and 33), 2′,4″-di-ASPM III (peaks 40, 34), 2′,3″,4″-tri-ASPM II (peaks 47 and 51) and 2′,3″,4″-tri-ASPM III (peaks 52 and 55) or their spatial isomers, respectively, which are intermediates in the synthesis of ASPM [1].

Compounds in peaks 30 ($[M+H]^+$ *m/z* 1029), 37 ($[M+H]^+$ *m/z* 1043), 49 ($[M+H]^+$ *m/z* 1071) and 54 ($[M+H]^+$ *m/z* 1085) were 60 u more than 2′,4″-di-ASPM II, 2′,4″-di-ASPM III, 2′,3″,4″-tri-ASPM II and 2′,3″,4″-tri-ASPM III, respectively. The $[M+H]^+$ CID spectra of these impurities are shown in Fig. 6. The fragmentation pathways are analogous to those in Fig. 5. Product ions, formed due to loss of 60 u, indicated that one of the double bonds at position C-10 to C-13 (α, β, γ, δ-unsaturated butadiene) had reacted with acetic acid. This was confirmed by LC with diode array detection where the characteristic absorbance of the α, β, γ, δ-unsaturated butadiene at 232 nm disappeared correspondingly. The exact location could not be determined due to insufficient fragmentation of the aglycone ring. This position will further be referred to as "P". The compounds in peaks 30, 37, 49 and 54 were established as P,2′,4″-tri-ASPM II, P,2′,4″-tri-ASPM III, P,2′,3″,4″-tetra-ASPM II and P,2′,3″,4″-tetra-ASPM III, respectively (see Fig. 7). To our knowledge, this is the first time such impurities are described.

Other process-related impurities with special structures (e.g. those with aberrant sugar residues) will be discussed in the following sections according to their structures.

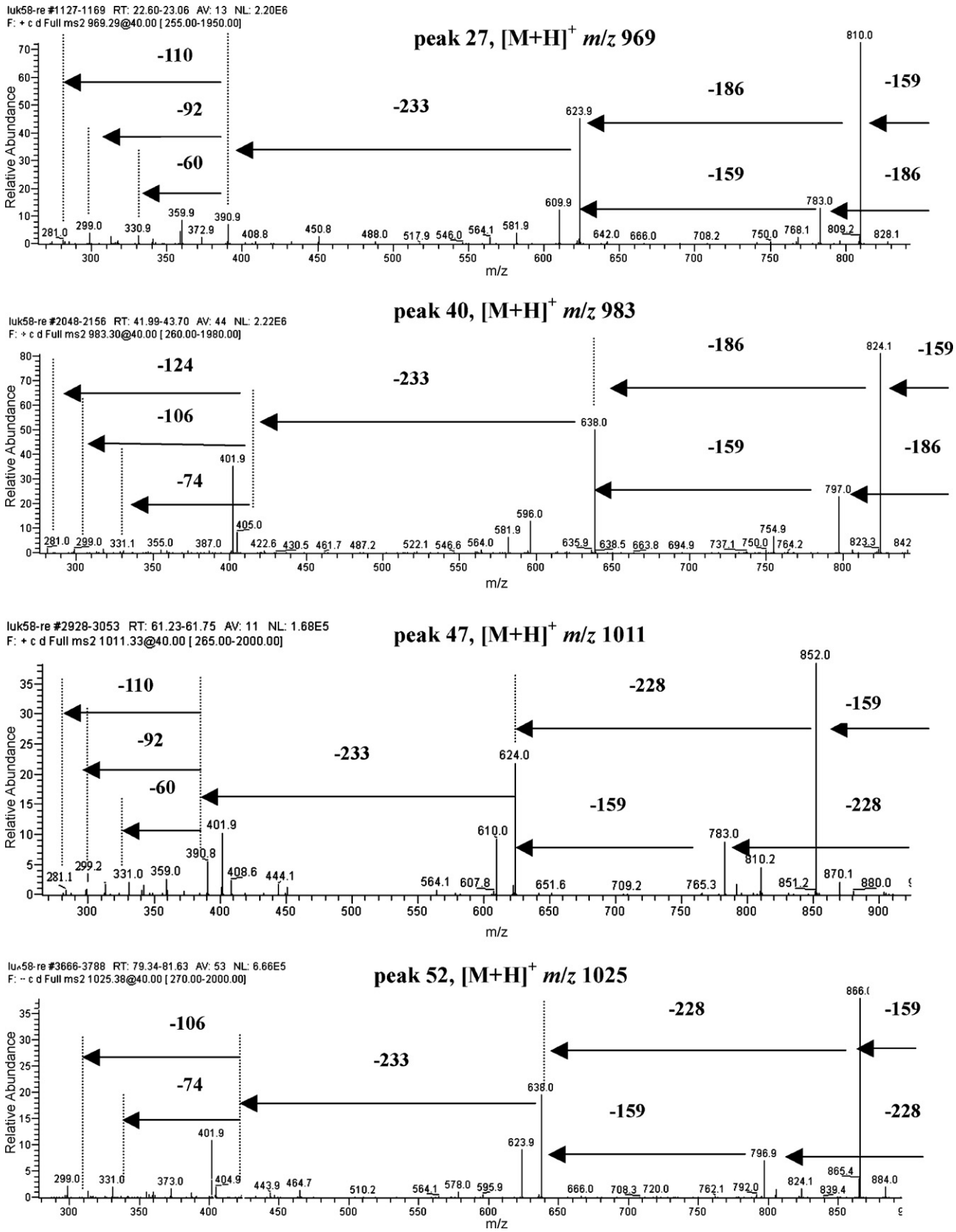

Fig. 5. $[M+H]^+$ CID spectra acquired for the compounds in peaks 27, 40, 47 and 52, the result of isolation and collisional activation of the precursor ion at *m/z* 969, 983, 1011 and 1025 (from top to bottom), respectively, in the ion trap at 40% CEL.

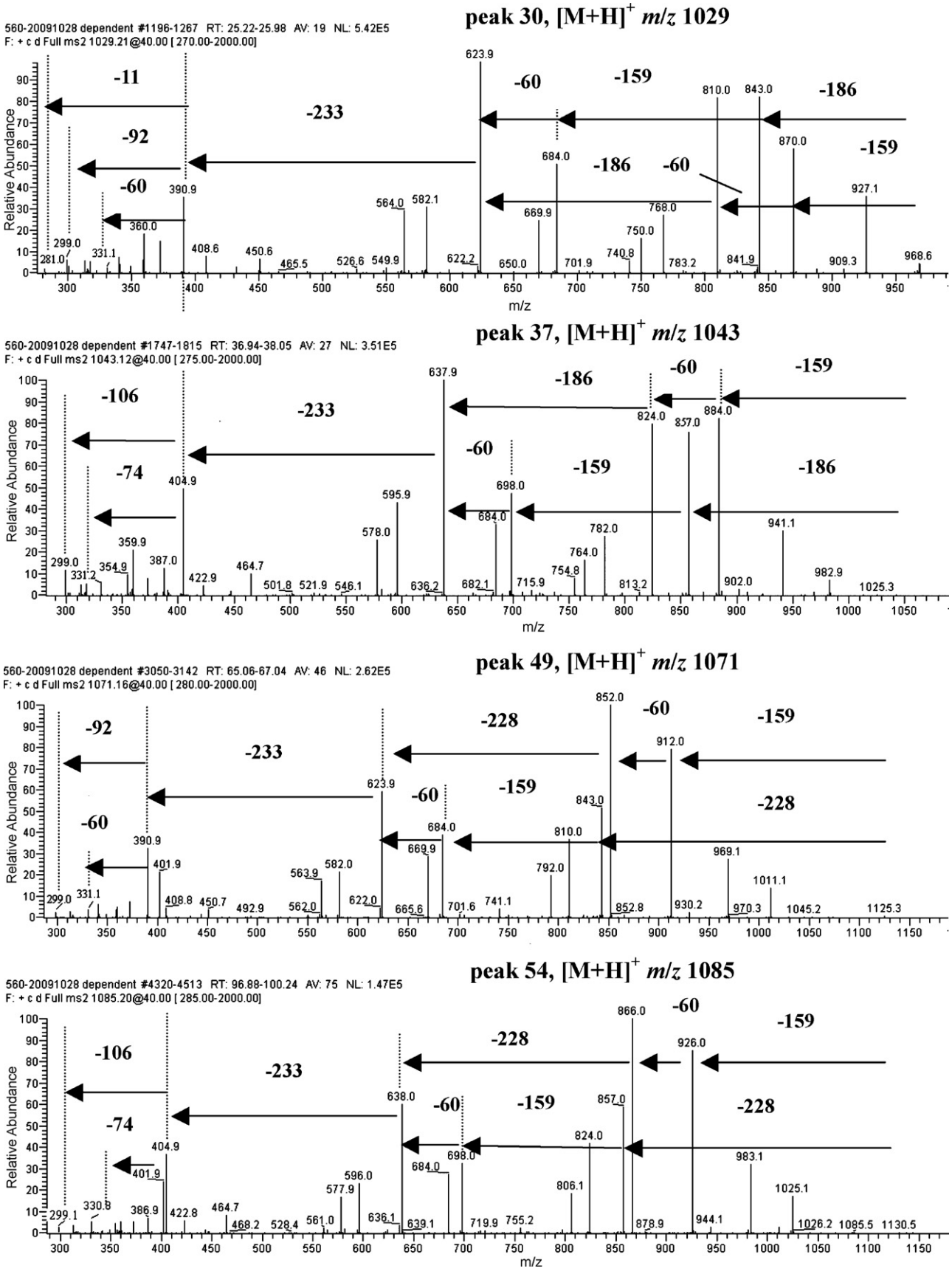

Fig. 6. $[M+H]^+$ CID spectra acquired for the compounds in peaks 30, 37, 49 and 54, the result of isolation and collisional activation of the precursor ion at *m/z* 1029, 1043, 1071 and 1085 (from top to bottom), respectively, in the ion trap at 40% CEL.

3.3.3. Impurities from degradation

Compounds corresponding to peak 1 ([M+H]$^+$ *m*/*z* 741) and peak 2 ([M+H]$^+$ *m*/*z* 755) were identified as NSPM II and NSPM III, respectively. The [M+H]$^+$ CID spectra of NSPM II followed the same pathway as that of SPM II, except the loss of 144 u which was not observed due to the lack of the mycarose in NSPM II. A similar phenomenon was observed for NSPM III.

In some samples, leucomycin A8 ([M+H]$^+$ *m*/*z* 786), meleumycin B2 ([M+H]$^+$ *m*/*z* 800) and 3″,4″-diacetyl leucomycin U ([M+H]$^+$ *m*/*z* 828, a newly identified impurity, which is a di-acetylated derivative of leucomycin U) were observed in peaks 11, 15 and 22, respectively. Their [M+H]$^+$ CID spectra followed similar fragmentation patterns as those of the major components, which reveal the presence of mono- (peaks 11, 15) or di-acetylated (peak 22) mycarose,

(A)

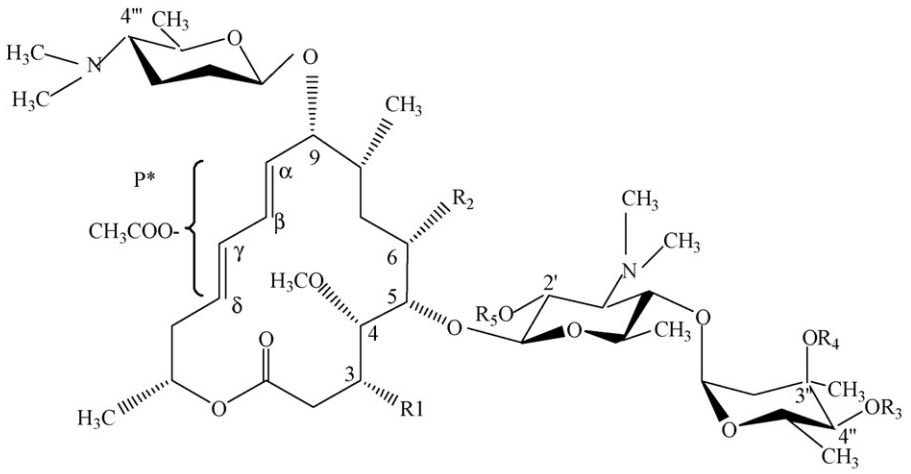

Proposed identification (peak No, [M+H]$^+$)	R_1	R_2	R_3	R_4	R_5	P*
3-*O*-butanoyl mono-ASPM (29, *m*/*z* 955)	$OCOCH_2CH_2CH_3$	CH_2CHO	$COCH_3$	H	H	−
3-*O*-butanoyl 3″,4″-di-ASPM (48, *m*/*z* 997)	$OCOCH_2CH_2CH_3$	CH_2CHO	$COCH_3$	$COCH_3$	H	−
3-*O*-butanoyl 2′,4″-di-ASPM (49, *m*/*z* 997)	$OCOCH_2CH_2CH_3$	CH_2CHO	$COCH_3$	H	$COCH_3$	−
3,4-anhydro mono-ASPM I (26, *m*/*z* 867)	− [1]	CH_2CHO	$COCH_3$	H	H	−
3,4-anhydro 3″,4″-di-ASPM I (42, *m*/*z* 909)	− [1]	CH_2CHO	$COCH_3$	$COCH_3$	H	−
3,4-anhydro 2′,4″-di-ASPM I (45, *m*/*z* 909)	− [1]	CH_2CHO	$COCH_3$	H	$COCH_3$	−
3,4-anhydro, 2′,3″,4″-tri-ASPM I (56, *m*/*z* 951)	− [1]	CH_2CHO	$COCH_3$	$COCH_3$	$COCH_3$	−
3,4-anhydro, P, 2′,3″,4″-tetra-ASPM I (56, *m*/*z* 1011)	− [1]	CH_2CHO	$COCH_3$	$COCH_3$	$COCH_3$	+ [2]
6-hydroxyethyl mono-ASPM III (9, *m*/*z* 943)	$OCOCH_2CH_3$	CH_2CH_2OH	$COCH_3$	H	H	−
6-hydroxyethyl 2′,4″-di-ASPM II (22, *m*/*z* 971)	$OCOCH_3$	CH_2CH_2OH	$COCH_3$	H	$COCH_3$	−
6-formyl mono-ASPM II (11, *m*/*z* 913)	$OCOCH_3$	CHO	$COCH_3$	H	H	−
6-carboxymethyl mono-ASPM III (12, *m*/*z* 957)	$OCOCH_2CH_3$	CH_2COOH	$COCH_3$	H	H	−
6-carboxymethyl di-ASPM III (24, *m*/*z* 999)	$OCOCH_2CH_3$	CH_2COOH	$COCH_3$	$COCH_3$	H	−
P, 2′,4″-tri-ASPM II (30, *m*/*z* 1029)	$OCOCH_3$	CH_2CHO	$COCH_3$	H	$COCH_3$	+ [2]
P, 2′,4″-tri-ASPM III (37, *m*/*z* 1043)	$OCOCH_2CH_3$	CH_2CHO	$COCH_3$	H	$COCH_3$	+ [2]
P, 2′,3″,4″-tetra-ASPM II (49, *m*/*z* 1071)	$OCOCH_3$	CH_2CHO	$COCH_3$	$COCH_3$	$COCH_3$	+ [2]
P, 2′,3″,4″-tetra-ASPM III (54, *m*/*z* 1085)	$OCOCH_2CH_3$	CH_2CHO	$COCH_3$	$COCH_3$	$COCH_3$	+ [2]

[1] Lack the R1 substituent and have a double bond between C-3 and C-4 whose stereochemistry will change correspondingly;

[2] One of the double bonds at position C-10 to C-13 (α, β, γ, δ-unsaturated butadiene) reacted with acetic acid, but the exact position of the substituent was not determined.

Fig. 7. Proposed structures for the impurities characterized in this work.

(B)

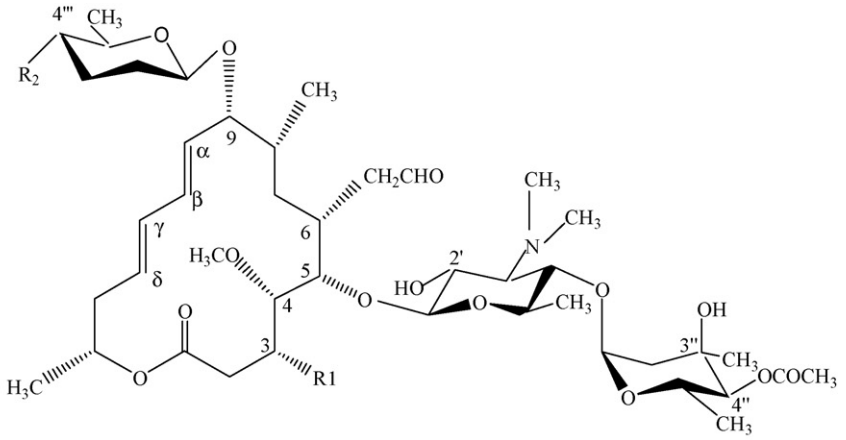

Identification (Peak No)	$[M+H]^+$	R_1	R_2
4′″-*N*,*N*-didemethyl mono-ASPM II (peak 4)	899	$OCOCH_3$	NH_2
4′″-*N*-demethyl mono-ASPM II (peak 5)	913	$OCOCH_3$	$NHCH_3$
4′″-*N*,*N*-didemethyl mono-ASPM III (peak 6)	913	$OCOCH_2CH_3$	NH_2
4′″-*N*-demethyl mono-ASPM III (peak 8)	927	$OCOCH_2CH_3$	$NHCH_3$

(C)

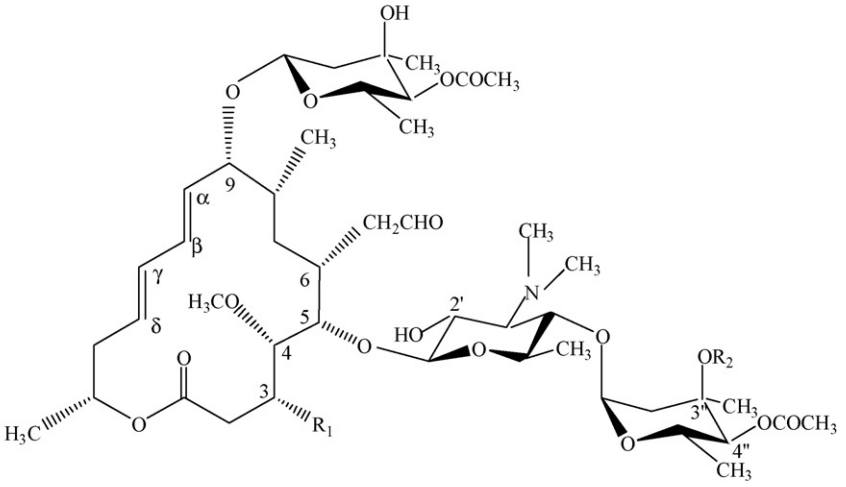

Proposed identification (Peak No.)	$[M+H]^+$	R_1	R_2
mono-ASPM II with aberrant forosaminyl (Mr 204) (Peak 28)	972	$OCOCH_3$	H
mono-ASPM III with aberrant forosaminyl (Mr 204) (Peak 36)	986	$OCOCH_2CH_3$	H
di-ASPM II with aberrant forosaminyl (Mr 204) (Peak 50)	1014	$OCOCH_3$	$COCH_3$
di-ASPM III with aberrant forosaminyl (Mr 204) (Peak 54)	1028	$OCOCH_2CH_3$	$COCH_3$

Fig. 7. (*Continued*)

mycaminose and the characteristic ions set of SPM II (peaks 11 and 22) and III (peak 15), respectively. However, instead of loss of 159 u (forosaminyl), loss of 18 u (water) was observed.

3.3.4. Impurities from other sources

3.3.4.1. Isomers of major components. As observed in other macrolide antibiotics [2,4,12], isomers of the major components with the same *m*/*z* values and similar product ions were also found in ASPM, e.g. isoforms of mono-ASPM II in peaks 4, 9, 11 and 14, isoforms of mono-ASPM III in peaks 6, 15, 18 and 19, isoforms of di-ASPM II in peaks 18 and 28, and isoforms of di-ASPM III in peaks 31, 35 and 37. All of them were co-eluted with other impurities. However, positional isomers and even spatial isomers cannot be distinguished by LC/MS only. Further NMR experiments are necessary to confirm these structures.

3.3.4.2. Related substances of ASPM with a different C-3 substituent (see Fig. 7A). The three impurities in peaks 29, 48 and 49 with $[M+H]^+$ *m*/*z* 955, 997 and 997, were characterized as 3-O-butanoyl mono-ASPM, 3-O-butanoyl 3″,4″-di-ASPM and 3-O-butanoyl 2′,4″-

(D)

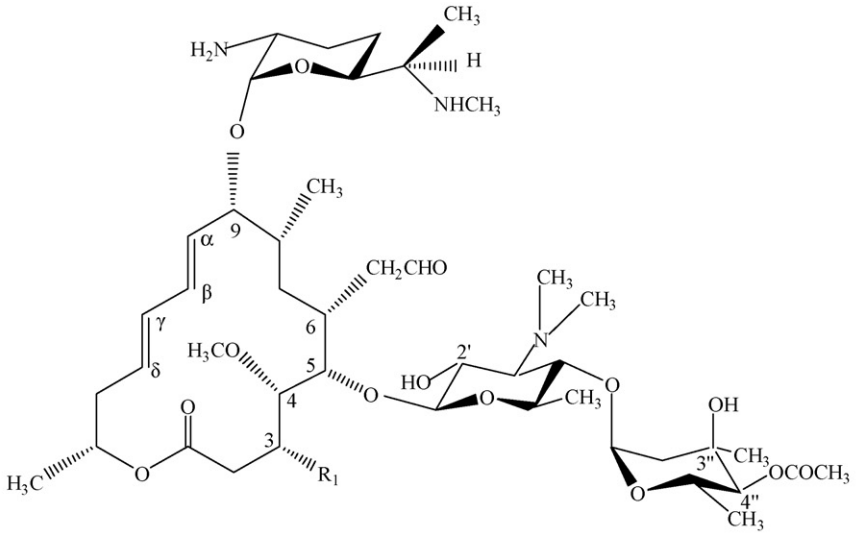

Proposed identification (Peak No.)	$[M+H]^+$	R_1
mono-ASPM II with aberrant forosaminyl (Mr 174) (Peak 46)	942	$OCOCH_3$
mono-ASPM III with aberrant forosaminyl (Mr 174) (Peak 53)	956	$OCOCH_2CH_3$
3,4-anhydro P, 4″-di-ASPM I with aberrant forosaminyl (Mr 174) (Peak 50)	942	– [1)]*

[1)]* Lack the R1 substituent and have a double bond between C-3 and C-4 whose stereochemistry will change correspondingly; with "P" structure at the aglycone ring.

(E)

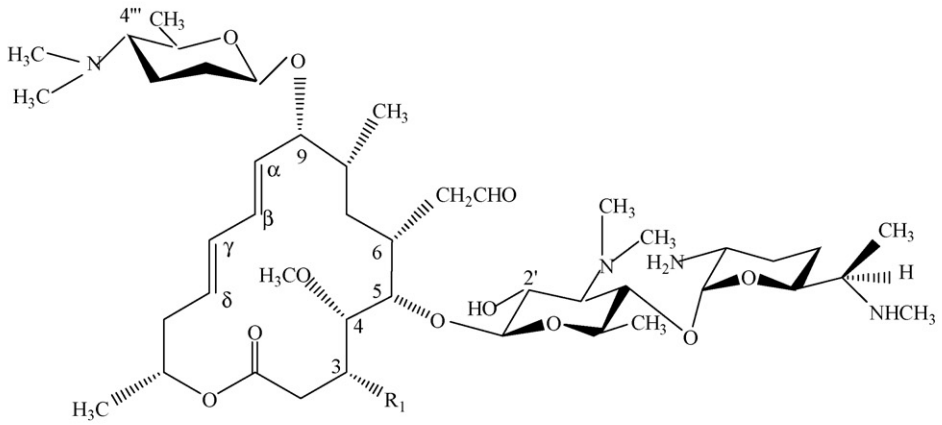

Proposed identification (Peak No.)	$[M+H]^+$	R_1
SPM II with aberrant mycarose (Mr 156) (Peak 17)	897	$OCOCH_3$
SPM III with aberrant mycarose (Mr 156) (Peak 22)	911	$OCOCH_2CH_3$

Fig. 7. (*Continued*).

di-ASPM, respectively. The loss of 88 u (corresponding to butanoic acid), 14 u higher than derivatives of SPM III, was observed at position C-3.

The protonated molecules for compounds in peaks 3 ($[M+H]^+$ m/z 681), 6, 9 and 26 ($[M+H]^+$ m/z 867), 42 ($[M+H]^+$ m/z 909), 45 ($[M+H]^+$ m/z 909) and 56 ($[M+H]^+$ m/z 951 and 1011) are 18 u less than NSPM I, mono-ASPM I (isoforms), 3″,4″-di-ASPM I, 2′,4″-di-ASPM I, 2′,3″,4″-tri-ASPM I and P,2′,3″,4″-tetra-ASPM I, respectively, and their corresponding product ions are all 18 u less. Unlike SPM I and its corresponding derivatives, further losses of water at C-3 were not observed. Based on the above observations and the literature [4,12], these impurities were suggested to be derivatives, which lack the R_1 substituent and have a double bond between C-3 and C-4 (3,4-anhydro). The stereochemistry will change accordingly.

3.3.4.3. Related substances of ASPM with a different C-6 substituent (see Fig. 7A). The $[M+H]^+$ CID spectra of the impurities in peaks 9 ($[M+H]^+$ m/z 943) and 22 ($[M+H]^+$ m/z 971) show product ions, 2 u higher than those of mono-ASPM III and 2′,4″-di-ASPM II, respectively. Based on the above information and the structures of SPM impurities [4], the impurities in peaks 9 and 22 were characterized

Table 1
List of major ASPM components, minor APIs and related substances in commercial ASPM samples.

Peak	$[M+H]^+$	Identification	Structure	Origin
1	741	NSPM II[c]	Fig. 1	Degradation
2	755	NSPM III[c]	Fig. 1	
3	681	3,4-Anhydro NSPM I[c]	Fig. 1	
4	927	Isoform 1 of mono-ASPM II[e]		Synthesis
	681	NSPM I with aberrant mycaminose (M_r 173)[e]		Starting material
	899	4‴-N,N-didemethyl mono-ASPM II[d]	Fig. 7B	[b]
5	913	4‴-N-demethyl mono-ASPM II[d]	Fig. 7B	[b]
6	941	Isoform 1 of mono-ASPM III[e]		Synthesis
	913	4‴-N,N-didemethyl mono-ASPM III[d]	Fig. 7B	[b]
	867	3,4-Anhydro mono-ASPM I (isoform)[e]		[b]
7	885	SPM II[c]	Fig. 1	Starting material
8	927	4‴-N-demethyl mono-ASPM III[d]	Fig. 7B	[b]
9	927	Isoform 2 of mono-ASPM II[e]		Synthesis
	943	6-Hydroxyethyl mono-ASPM III[d]	Fig. 7A	[b]
	867[a]	3,4-Anhydro mono-ASPM I (isoform)[e]		[b]
10	899	SPM III[c]	Fig. 1	Starting material
11	913	6-Formyl mono-ASPM II[d]	Fig. 7A	[b]
	927	Isoform 3 of mono-ASPM II[e]		Synthesis
	786[a]	Leucomycin A8[c]	Fig. 1	Degradation
12	957	6-Carboxymethyl mono-ASPM III[d]	Fig. 7A	[b]
13	885	Mono-ASPM I[c]	Fig. 1	Minor API
14	927	Isoform 4 of mono-ASPM II[e]		Synthesis
	825	Mono-ASPM I with aberrant mycaminose (M_r 173)[e]		[b]
15	800[a]	Meleumycin B2[c]	Fig. 1	Degradation
	941	Isoform 2 of mono-ASPM III[e]		Synthesis
	955	Mono-ASPM II with aberrant forosaminyl (M_r 187)[e]		[b]
16	**927**	**Mono-ASPM II**	Fig. 1	**Major API**
17	897	SPM II with aberrant mycarose (M_r 156)[d]	Fig. 7E	Starting material
	924	Mono-ASPM II with aberrant mycaminose (M_r 173) and an additional $-NH_2$ on the aglycone ring[e]		[b]
18	941	Isoform 3 of mono-ASPM III[e]		Synthesis
	969	Isoform 1 of di-ASPM II[e]		Synthesis
19	969	Mono-ASPM III with aberrant forosaminyl (M_r 187) (isoform)[e]		[b]
	941	Isoform 4 of mono-ASPM III[e]		Synthesis
20	**941**	**Mono-ASPM III**	Fig. 1	**Major API**
21	938	Mono-ASPM III with aberrant mycaminose (M_r 173) and an additional $-NH_2$ on the aglycone ring[e]		[b]
22	828[a]	3″,4″-diacetyl leucomycin U[d]		[b]
	911	SPM III with aberrant mycarose (M_r 156)[d]	Fig. 7E	Starting material
	971	6-Hydroxyethyl 2′,4″-di-ASPM-II[d]	Fig. 7A	[b]
23	969	Mono-ASPM III with aberrant forosaminyl (M_r 187) (isoform)[e]		[b]
24	999	6-Carboxymethyl di-ASPM III[d]	Fig. 7A	[b]
25	927	Di-ASPM I[c]	Fig. 1	Minor API
	895	3,4-Anhydro mono-SPM I with aberrant forosaminyl (M_r 187)[e]		[b]
26	867	3,4-Anhydro mono-ASPM I (major impurity)[d]	Fig. 7A	[b]
27	969	2′,4″-Di-ASPM-II[c]	Fig. 1	Synthesis
28	972	Mono-ASPM II with aberrant forosaminyl (M_r 204)[d]	Fig. 7C	[b]
	969	Isoform 2 of di-ASPM II[e]		Synthesis
29	955	3-O-butanoyl mono-ASPM[d]	Fig. 7A	[b]
30	1029	P,2′,4″-tri-ASPM II[d]	Fig. 7A	Synthesis
	985[a]	6-Hydroxyethyl P,4″-di-ASPM-III with aberrant mycaminose (M_r 173)[e]		[b]
31	997	Di-ASPM II with aberrant forosaminyl (M_r 187)[e]		[b]
	983	Isoform 1 of di-ASPM III[e]		Synthesis
32	**969**	**Di-ASPM II**	Fig. 1	**Major API**
33	969	2′,4″-Di-ASPM-II[c]	Fig. 1	Synthesis
34	983	2′,4″-Di-ASPM-III[c]	Fig. 1	Synthesis
35	983	Isoform 2 of di-ASPM III[e]		Synthesis
	911[a]	6-hydroxyethyl mono-ASPM-II with aberrant mycaminose (M_r 173)[e]		[b]
36	986	Mono-ASPM III with aberrant forosaminyl (M_r 204)[d]	Fig. 7C	[b]
37	1043	P,2′,4″-tri-ASPM III[d]	Fig. 7A	Synthesis
	983	Isoform 3 of di-ASPM III[e]		Synthesis
38	1011	Di-ASPM III with aberrant forosaminyl (M_r 187)[e]		[b]
39	**983**	**Di-ASPM III**	Fig. 1	**Major API**
40	983	2′,4″-Di-ASPM III[c]	Fig. 1	Synthesis
41	909	3″,4″-Di-ASPM I with aberrant mycaminose (M_r 173)[e]		[b]
42	909	3,4-Anhydro 3″,4″-di-ASPM I[d]	Fig. 7A	[b]
43	969	P,3″,4″-tri-ASPM I with aberrant mycaminose (M_r 173)[e]		[b]
44	937	3,4-Anhydro 3″,4″-di-ASPM I with aberrant forosaminyl (M_r 187)[e]		[b]
45	909	3,4-Anhydro 2′,4″-di-ASPM I[d]	Fig. 7A	[b]
46	942	Mono-ASPM II with aberrant forosaminyl (M_r 174)[d]	Fig. 7D	[b]
47	1011	2′,3″,4″-Tri-ASPM II[c]	Fig. 1	Synthesis
48	997	3-O-butanoyl 3″,4″-di-ASPM[d]	Fig. 7A	[b]
49	1071	P,2′,3″,4″-tetra-ASPM II[d]	Fig. 7A	Synthesis
	997	3-O-butanoyl 2′,4″-di-ASPM[d]	Fig. 7A	[b]
50	1014	Di-ASPM II with aberrant forosaminyl (M_r 204)[d]	Fig. 7C	[b]
	942	3,4-Anhydro P,4″-di-ASPM I with aberrant forosaminyl (M_r 174)[d]	Fig. 7D	[b]

Table 1 (*Continued*)

Peak	$[M+H]^+$	Identification	Structure	Origin
51	1011[a]	2′,3″,4″-Tri-ASPM II[c]	Fig. 1	Synthesis
52	1025	2′,3″,4″-Tri-ASPM III[c]	Fig. 1	Synthesis
53	956	Mono-ASPM III with aberrant forosaminyl (M_r 174)[d]	Fig. 7D	[b]
54	1085	P,2′,3″,4″-tetra-ASPM III[d]	Fig. 7A	Synthesis
	1028	Di-ASPM III with aberrant forosaminyl (M_r 204)[d]	Fig. 7C	[b]
55	1025	2′,3″,4″-Tri-ASPM III[c]	Fig. 1	Synthesis
	969	Di-ASPM III with aberrant mycaminose (M_r 173) and its α, β, γ, δ-unsaturated butadiene saturated[e]		[b]
56	951	3,4-Anhydro 2′,3″,4″-tri-ASPM I[d]	Fig. 7A	[b]
	1011	3,4-Anhydro P,2′,3″,4″-tetra-ASPM I[d]	Fig. 7A	[b]

[a] Only exists in some samples.
[b] Acetylation derivatives of the impurities from starting materials; possible structures of the aberrant sugar residues are discussed in the text, and some of the proposed structures are shown in Fig. 7.
[c] Known components or impurities (total: 17).
[d] Newly identified impurities (total: 31).
[e] Partially identified impurities (total: 31); major components (total: 4) are shown in boldface.

as 6-hydroxyethyl mono-ASPM III and 6-hydroxyethyl 2′,4″-di-ASPM II, respectively.

Based on similar observations, the compound in peak 11 ($[M+H]^+$ m/z 913) was identified as 6-formyl mono-ASPM II, whose product ions were all 14 u less than those of mono-ASPM II. The compounds in peaks 12 ($[M+H]^+$ m/z 957) and 24 ($[M+H]^+$ m/z 999) were identified as 6-carboxymethyl mono-ASPM III and 6-carboxymethyl di-ASPM III, whose product ions were all 16 u more than those of mono-ASPM III and di-ASPM III, respectively. In some samples, minor impurities 6-hydroxyethyl P,4″-di-ASPM III ($[M+H]^+$ m/z 985) with an aberrant mycaminose (M_r 173) and 6-hydroxyethyl mono-ASPM II ($[M+H]^+$ m/z 911) with an aberrant mycaminose (M_r 173) were observed in peaks 30 and 35, respectively.

3.3.4.4. Related substances of ASPM with different sugar residues. Many impurities were observed with different sugar residues in the samples. For example, the molecular masses in peaks 5 ($[M+H]^+$ m/z 913) and 8 ($[M+H]^+$ m/z 927) are 14 u less than mono-ASPM II and mono-ASPM III, respectively. MS^2 investigation of these compounds showed product ions and losses, identical to those of mono-ASPM II and mono-ASPM III, except for the initial loss corresponding to forosaminyl. A loss of 145 u is observed instead of 159 u, which indicates that these impurities have an aberrant forosamine sugar. For SPM, the difference of 14 u was attributed to a difference in the degree of methylation of the amino group [4]. Thus, the compounds in peaks 5 and 8 were identified as 4‴-N-demethyl mono-ASPM II and 4‴-N-demethyl mono-ASPM III, respectively. Similarly, the impurities in peaks 4 ($[M+H]^+$ m/z 899) and 6 ($[M+H]^+$ m/z 913) were identified as 4‴-N,N-didemethyl mono-ASPM II and 4‴-N,N-didemethyl mono-ASPM III, where protonated molecules are 28 u less than mono-ASPM II and mono-ASPM III, respectively (see Fig. 7B).

Other compounds with aberrant forosaminyl sugar are described below. These impurities are classified into three groups based on the initial loss.

(1) *Loss of 204*: the fragmentation of impurities in peaks 28 ($[M+H]^+$ m/z 972), 36 ($[M+H]^+$ m/z 986), 50 ($[M+H]^+$ m/z 1014) and 54 ($[M+H]^+$ m/z 1028) are similar to mono-ASPM II, III, di-ASPM II and III, respectively, except that an initial loss of 204 u instead of 159 u was observed. The initial loss of 204 may be due to the replacement of forosaminyl with mono-acetylated mycarose (the cleavage of the glycosidic bond takes place at the aglycone side, i.e. 186 u + 18 u). Hence these impurities might be the modified form of the above mentioned compounds with mono-acetylated mycarose at position C-9. Proposed structures are shown in Fig. 7C.

(2) *Loss of 174*: similarly, an initial loss of 174 u (156 u + 18 u) was observed for impurities in peaks 46 ($[M+H]^+$ m/z 942), 50 ($[M+H]^+$ m/z 942) and 53 ($[M+H]^+$ m/z 956). Their remaining fragmentations are similar to those of mono-ASPM II, 3,4-anhydro P,4″-di-ASPM I and mono-ASPM III, respectively. The aberrant forosaminyl sugar may be purpurosamine (M_r 174). Fig. 7D shows the proposed structures.

(3) *Loss of 187*: impurities in peaks 25 ($[M+H]^+$ m/z 895), 44 ($[M+H]^+$ m/z 937), 15 ($[M+H]^+$ m/z 955), 19 and 23 ($[M+H]^+$ m/z 969), 31($[M+H]^+$ m/z 997) and 38 ($[M+H]^+$ m/z 1011) showed an initial loss of 187 u and their remaining fragmentations are similar to 3,4-anhydro mono-ASPM I, 3,4-anhydro 3″,4″-di-ASPM I, mono-ASPM II, mono-ASPM III (isoforms), di-ASPM II and di-ASPM III, respectively. The aberrant sugar (M_r 187) is 28 u higher than forosaminyl, which might be N,N-didemethyl-diethyl or N-methyl, N-propyl forosaminyl.

Similar to the above observations, compounds in peaks 17 ($[M+H]^+$ m/z 897) and 22 ($[M+H]^+$ m/z 911) were identified as related substances of SPM-II and SPM-III with aberrant mycarose (M_r 156, the cleavage of the disaccharide bond takes place at the mycarose side), which may be purpurosamine. Their proposed structures are also shown in Fig. 7E.

Similarly, aberrant mycaminose (M_r 173) was observed for impurities in: (a) peaks 4 ($[M+H]^+$ m/z 681), 14 ($[M+H]^+$ m/z 825), 41 ($[M+H]^+$ m/z 909) and 43 ($[M+H]^+$ m/z 969) which were the modified forms of NSPM I, mono-ASPM I, di-ASPM I and P,3″,4″-tri-ASPM I, respectively; (b) peaks 17 ($[M+H]^+$ m/z 924) and 21 ($[M+H]^+$ m/z 938) which were modified mono-ASPM II and mono-ASPM III with an additional $-NH_2$ substitutent on the aglycone ring (further investigation by NMR is needed to determine the exact position); (c) peak 55 ($[M+H]^+$ m/z 969) which was modified di-ASPM III with its α, β, γ, δ-unsaturated butadiene in the aglycone ring saturated. The aberrant mycaminose (M_r 173) might be the dehydrated form of mycaminose (M_r 191) or a modified form of forosaminyl (M_r 159) where one of the N-methyls was replaced by N-ethyl.

Due to lack of further information about the sugar moieties, additional NMR experiments are necessary to confirm the above aberrant sugar groups.

4. Conclusion

The LC/MS^n investigation revealed the complexity of the ASPM samples. Using the Chinese Pharmacopoeia LC method, a total of 83 compounds were detected in 56 peaks (see overview in Table 1), whereas in LC–UV only 36 peaks were detected. It shows the importance of LC/MS in processing and quality control of pharmaceutical products.

Along with 31 newly identified impurities (Fig. 7A–E), 17 known related substances (Fig. 1) were traced. Due to lack of more information about aglycone and sugar moieties, 31 partially characterized impurities still would need further investigation by NMR. All impurities detected have a structure that is closely related to the main components. Most impurities in commercial ASPM arise from the starting materials (including their co-existing related substances, e.g. those with aberrant sugars) and the synthesis process (including side products at α, β, γ, δ-unsaturated butadiene), and the major impurity in the samples investigated is 3,4-anhydro mono-ASPM I (peak 26).

References

[1] X.P. Liu, J. Xiangtan, Min. Institut. 12 (1997) 65.
[2] M. Hu, C.Q. Hu, Anal. Chim. Acta 535 (2005) 89.
[3] X.G. Shi, S.Q. Zhang, J.P. Fawcett, D.F. Zhong, J. Pharm. Biomed. Anal. 36 (2004) 593.
[4] M. Pendela, C. Govaerts, J. Diana, J. Hoogmartens, A. Van Schepdael, E. Adams, Rapid Commun. Mass Spectrom. 21 (2007) 599.
[5] A. Kondo, T. Nakatani, Y. Kuzuya, H. Suzuki, H. Sano, K. Yamaguchi, K. Shirahata, K. Takahashi, K. Kita, Y. Nishiie, Jpn. J. Antibiot. 43 (1990) 1152.
[6] A. Kondo, K. Sato, K. Shuto, K. Yamashita, S. Ichikawa, K. Takahashi, K. Kita, Y. Nishiie, H. Sano, K. Yamaguchi, Jpn. J. Antibiot. 43 (1990) 1521.
[7] S.Y. Li, D.S. Nelson, Int. J. Immunopharmacol. 7 (1985) 881.
[8] H. Takahashi, K. Yoshida, T. Matsuda, H. Komatsu, K. Toyoda, M. Morita, O. Nuka, N. Sera, Jpn. J. Antibiot. 34 (1981) 1082.
[9] Z.H. Song, C.N. Wang, Mikrochim. Acta 149 (2005) 117.
[10] F.M. Espinas, Y. Odakura, N. Suzuki, H. Sasaki, Jpn. J. Antibiot. 34 (1981) 1141.
[11] The State Pharmacopoeia Commission of PR China, Pharmacopoeia of the People's Republic of China, Edition 2005, Chemical Industry Press, Beijing, 2005, p. 6.
[12] C. Govaerts, H.K. Chepkwony, A. Van Schepdael, E. Adams, E. Roets, J. Hoogmartens, J. Mass Spectrom. 39 (2004) 437.